Medicinal Chemistry Research (2019) 28:1773–1782
https://doi.org/10.1007/s00044-019-02414-5

MEDICINAL
CHEMISTRY
RESEARCH

ORIGINAL RESEARCH

New histone deacetylase inhibitors and anticancer agents from *Curcuma longa*

Pakit Kumboonma[1] · Thanaset Senawong[2] · Somprasong Saenglee[2] · Gulsiri Senawong[2] · La-or Somsakeesit[1] · Chavi Yenjai[1] · Chanokbhorn Phaosiri[1]

Received: 30 May 2019 / Accepted: 23 July 2019 / Published online: 4 August 2019

Abstract

The aims of this study were to explore histone deacetylase inhibitory and antioxidant activities of curcuminoids as well as derivatives of curcumin. Curcumin (**6**), demethoxycurcumin (**7**), dihydrocurcumin (**8**), bisdemethoxycurcumin (**9**), and hydroxycurcumin (**10**) were isolated and tested against histone deacetylases in HeLa nuclear extract. Hydroxycurcumin (**10**) showed the best inhibition among the isolated compounds. Some curcumin derivatives were also prepared and tested. The potential derivatives were tested on five cancer cell lines. All compounds exhibited slightly weaker antiproliferative activities against cancer cells and less toxic to non-cancer cells than curcumin (**6**). The least toxic derivative (**17**) exhibited the best antiproliferative activity against human cervical cancer cell lines (HeLa) with the IC_{50} value of 4.69 ± 0.14 µM. The most active histone deacetylase inhibitor (**19**) showed the highest potency against human colon cancer cell lines (HCT116) and the selective binding to HDAC4 based on molecular docking experiments. Most derivatives possessed antioxidant activities superior to curcumin. The results suggested potential candidates for anticancer agents.

Keywords Turmeric · Curcumin · HeLa cell · Anticancer · Molecular docking

Introduction

Acetylation and deacetylation of histone proteins play important roles in the epigenetic regulation of transcription in cells. Many disorders and metabolic diseases occur by perturbation of the balance between histone acetyltransferases (HATs) and histone deacetylases (HDACs) (Konstantinopoulos et al. 2007; Weichert 2009). HDACs have an important effect on gene transcription, differentiation, apoptosis, and tumorigenesis. Therefore, HDACs have been validated as prominent therapeutic targets for a broad range of human disorders such as cancer, diabetes, and brain disorders (Paris et al. 2008; Noh et al. 2009; Bertrand 2010; Manal et al. 2016). In humans, HDACs are divided into four classes based on their homology to yeast models, subcellular localization and enzymatic activities. Eighteen mammalian isoforms of HDACs have been reported (Micelli, Rastelli 2015). Class I (HDAC1, 2, 3, and 8), class IIa (HDAC4, 5, 7, and 9), class IIb (HDAC6 and 10) and class IV (HDAC11) HDACs are zinc-ion-dependent metallo proteins. Class III (SIRT1-7) HDACs are zinc-ion-independent and NAD^+-dependent proteins. The different isoforms are mainly found in diverse diseases such as cancer cells.

HDAC inhibitors (HDACi) have been reported and categorized into five groups according to their chemical structures including hydroxamic acid derivatives, cyclic tetrapeptides, benzamides, electrophilic ketones, and carboxylic acids (Miller et al. 2003; Zhang et al. 2012; Ravichandiran et al. 2015). In spite of the diverse structures, the pharmacophore of most HDAC inhibitors consists of three parts including a zinc-binding group, a hydrophobic linker, and a surface recognition area. Up to now, the hydroxamic

---

Supplementary information The online version of this article (https://doi.org/10.1007/s00044-019-02414-5) contains supplementary material, which is available to authorized users.

✉ Chanokbhorn Phaosiri
chapha@kku.ac.th

[1] Natural Products Research Unit, Center of Excellence for Innovation in Chemistry, Ministry of Higher Education, Science, Research and Innovation (Implementation Unit-IU, Khon Kaen University), Department of Chemistry, Faculty of Science, Khon Kaen University, Khon Kaen 40002, Thailand

[2] Natural Products Research Unit, Department of Biochemistry, Faculty of Science, Khon Kaen University, Khon Kaen 40002, Thailand

acids have been reported to be the most potent group of HDAC inhibitors of which suberoylanilide hydroxamic acid (**1**, SAHA, Vorinostat), Belinostat, Chidamide and Panobinostat approved by the FDA for the treatment of lymphoma or myeloma (Mann et al. 2007; Banerjee et al. 2019). However, the highly potent hydroxamic compounds typically possess serious toxicities and poor metabolic stabilities (Hahnen et al. 2008; Suzuki and Miyata 2005). Moreover, these compounds also nonspecifically inhibit all HDAC isoforms. All of these broad spectrum HDAC inhibitors cause similar adverse effects such as fatigue, nausea, and vomiting (Ontoria et al. 2009). Therefore, development of novel HDAC inhibitors with safe, isoform-selective and low toxicity still remain as a challenge research. A variety of non-hydroxamic acids, for examples, hydroxycapsaicin (**2**), [6]-gingerol (**3**), [6]-shogaol (**4**), demethylated-[6]-shogaol (**5**), and curcumin (**6**) have been investigated as HDAC inhibitors as shown in Figs 1 and 2 (Senawong et al. 2015; Kumboonma et al. 2017; Tatar et al. 2009). Even though their HDAC inhibitory activities are not comparable to those of SAHA (**1**, $IC_{50} = 110–370$ nM) (Gopalan et al. 2013), one of these compounds, hydroxycapsaicin (**2**) is accepted as a good inhibitor with low toxicities towards normal cells.

Turmeric (*Curcuma longa*) is a rhizomatous perennial plant of the ginger family. The rhizome of *C. longa* has been used in indigenous medicine for the treatment of inflammatory disorders. The major product from *C. longa*, curcumin (**6**) is reported to have many interesting biological activities including antioxidant (Ruby et al. 1995; Selvam et al. 2005), antimycobacterial (Changtam et al. 2010), anti-inflammatory (Chan et al. 1995), anticancer (Inano et al. 2000; Thapliyal, Maru 2001), anti-acetylcholinesterase (Premanand et al. 2009), and anti-HIV activities (Mazumder et al. 1995). However, several drawbacks of curcumin come from low aqueous solubility, low absorption, and poor bioavailability (Anand et al. 2008).Various structural modification of curcumin have been carried out in order to improve its bioavailability and activities (Khalil et al. 2014; Ahsan et al. 2015; Sharma et al. 2015; Puneeth et al. 2016). Curcumin can act as a good HDAC inhibitor with the IC_{50} value as 115 µM (Tatar et al. 2009). Nevertheless, there was no report regarding HDAC inhibitory activities of curcumin derivatives.

In our previous report, the [6]-shogaol (**4**) and its derivatives showed good HDAC inhibitory activities (Kumboonma et al. 2017). From the similar structure of [6]-shogaol (**4**) to curcumin (**6**), the semi-synthetic derivatives

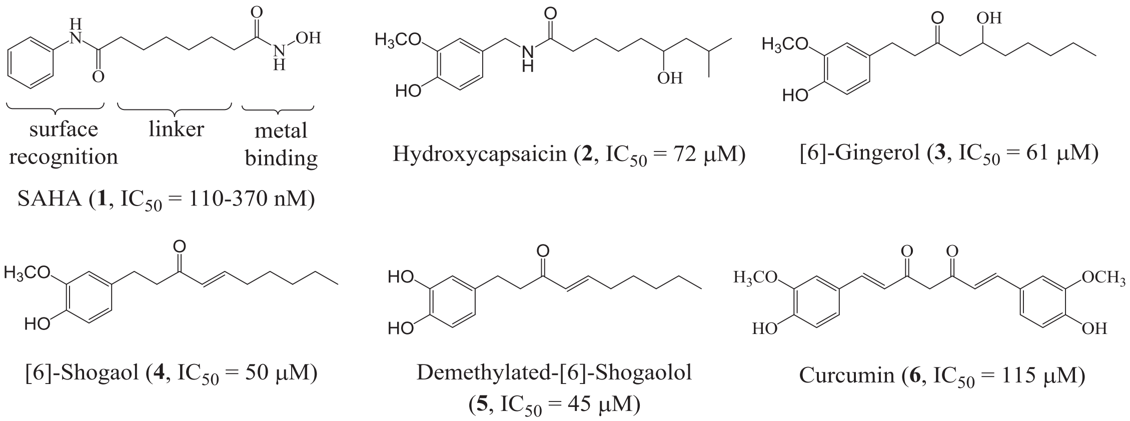

SAHA (**1**, IC_{50} = 110-370 nM)

Hydroxycapsaicin (**2**, IC_{50} = 72 µM)

[6]-Gingerol (**3**, IC_{50} = 61 µM)

[6]-Shogaol (**4**, IC_{50} = 50 µM)

Demethylated-[6]-Shogaolol (**5**, IC_{50} = 45 µM)

Curcumin (**6**, IC_{50} = 115 µM)

Fig. 1 Structures and IC_{50} values of known histone deacetylase inhibitors

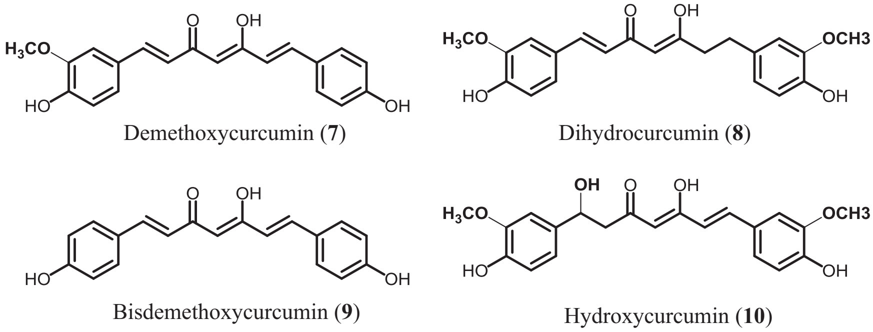

Demethoxycurcumin (**7**)

Dihydrocurcumin (**8**)

Bisdemethoxycurcumin (**9**)

Hydroxycurcumin (**10**)

Fig. 2 Structures of minor phenolic compounds from *Curcuma longa*

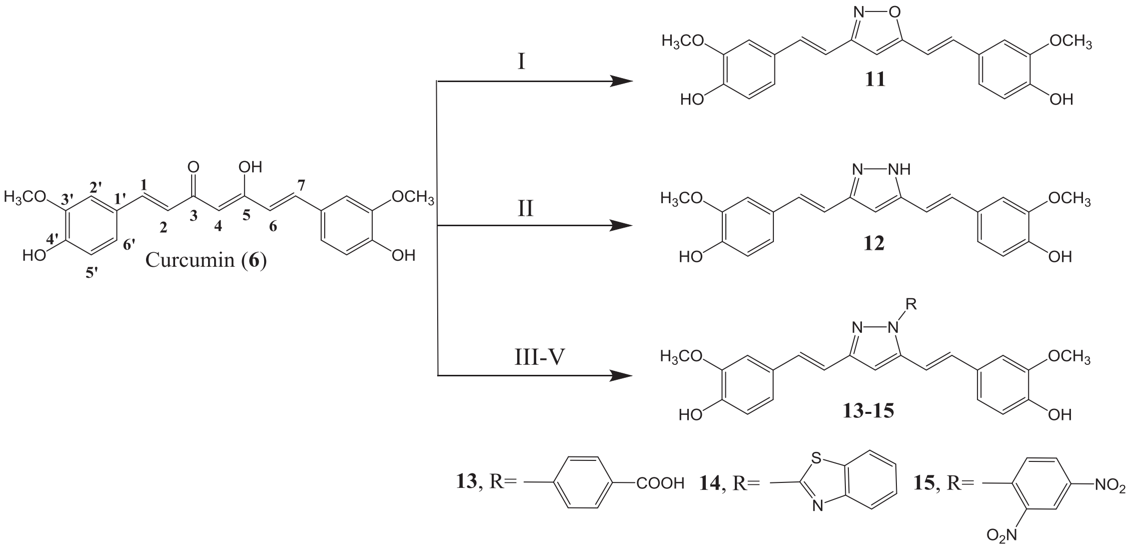

Scheme 1 Synthesis of isoxazole, pyrazole, and N-(substituted) pyrazole derivatives of curcumin. Reagents and conditions: (I) $NH_2OH\cdot HCl$, reflux, 6 h; (II) hydrazine hydrate, reflux, 8 h; (III) 4-hydrazinobenzoic acid hydrochloride, reflux, 8 h; (IV) 2-hydrazino benzothiazole, reflux, 8 h; and (V) 2,4-dinitrophenylhydrazine reflux, 8 h

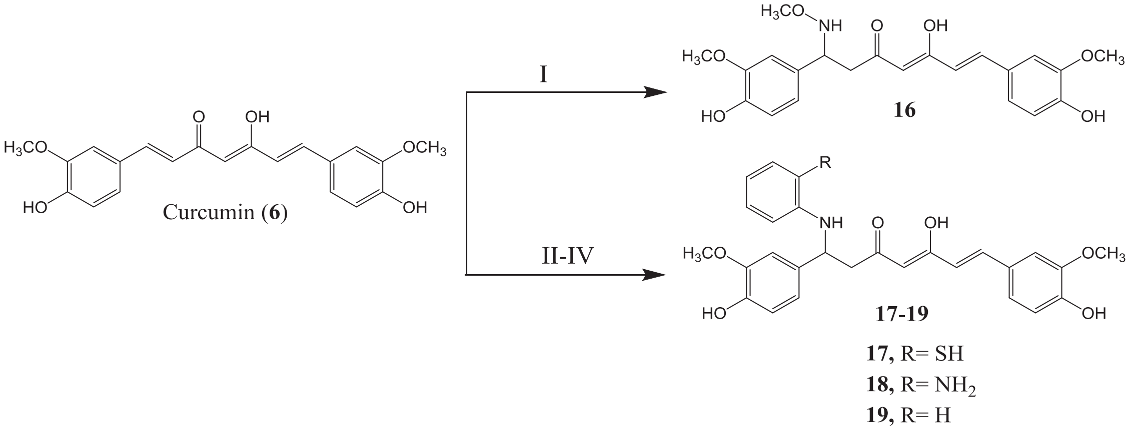

Scheme 2 Synthesis of amino derivatives of curcumin. Reagents and conditions: (I) $NH_2OCH_3\cdot HCl$, reflux, 6 h; (II) 2-aminothiophenol, reflux, 6 h; (III) *o*-phenylenediamine, reflux, 6 h; and (IV) aniline reflux, 6 h

of curcumin (**6**) were further investigated in this work. Molecular docking study, antiproliferative and antioxidant activities of all compounds were also carried out to extend the therapeutic potential.

Results and discussion

Curcumin (**6**) as the major product along with four minor phenolic compounds were extracted from the dried rhizome powder of turmeric. The isoxazole and pyrazole derivatives of curcumin were synthesized as depicted in Scheme 1. The amino derivatives of curcumin were prepared according to Scheme 2 by reacting curcumin (**6**) with methylamine hydrochloride, 2-aminothiophenol, *o*-phenylenediamine, and aniline to yield amino derivatives **16–19**, respectively.

Table 1 HDAC inhibitory activity of compounds at 100 µM

Compounds	%HDAC inhibition	Compounds	%HDAC inhibition
6	62	**13**	64
7	65	**14**	67
8	61	**15**	65
9	67	**16**	72
10	76	**17**	73
11	54	**18**	69
12	51	**19**	82

All compounds were initially screened at 100 µM, using the Fluor-de-Lyse™ in vitro fluorescence activity assay kit and measuring total HDAC activity in HeLa nuclear extract. The results are illustrated in Table 1. Among the natural products, hydroxycurcumin (**10**) possessed the best % HDAC inhibition value of 76%. Incorporation of functional groups with strong interactions such as hydrogen bond, π–π, and hydrophilic interactions can increase the binding affinity between inhibitor and enzyme. Therefore, the isoxazole, pyrazole, and amino derivatives of curcumin were designed and synthesized to improve the inhibitor-enzyme binding efficiency via additional hydrogen bonds and coordination to the zinc ion. No significant improvement was observed from the isoxazole derivative **11** and the pyrazole derivative **12**. However, the pyrazole derivatives with *N*-aromatic substitution **13–15** led to a moderately increased activity as compared to curcumin, whereas the amino derivatives of curcumin **16–19** showed a significantly increased inhibition. The most active compound among the amino derivatives of curcumin was **19** which contained a phenylamino group at the Michael acceptor position of curcumin with %HDAC inhibition of 82%.

In order to rationalize the in vitro results and to explore a possibility of being HDAC isoform-selective inhibitors, the selected compounds, curcumin (**6**), hydroxycurcumin (**10**), and **19** were docked into the catalytic pockets of the representative isoform of class I (HDAC2 and HDAC8) and Class II (HDAC4 and HDAC7). The in silico results are summarized in Table 2. The molecular docking method was validated in all isoforms through the re-docking of SAHA and TSA within the protein structures. In comparison to curcumin (**6**), hydroxycurcumin (**10**) possessed the lowest inhibition constant against HDAC2 (K_i of **10** = 0.98 μM). In addition to coordination towards the zinc ion, the hydrophilic interaction occurs between the methoxy group of **10** and the carbonyl group of Gly142 as shown in Fig. 3a. Another binding is the close π–π stacking interaction between the phenyl ring of **10** and Phe210. The previous study indicated that HDAC2 are overexpressed in the cortex and hippocampus of Alzheimer's disease patients (Hu et al. 2018). Therefore, hydroxycurcumin (**10**) can be an attractive candidate for the treatment of neurodegenerative diseases. Compound **19** showed the highest selectivity against HDAC4 (K_i of **19** = 2.11 μM). The binding mode of **19** in the HDAC4 binding cavity is depicted in Fig. 3b. The major interaction between HDAC4 and compound **19** is the coordination of the hydroxy group to the zinc ion with a distance of 3.03 Å. Moreover, compound **19** binds to HDAC4 via three hydrogen bonds. The hydrogen bonds occur between the hydroxy group of **19** and the amino group of Lys20 (2.16 Å) as well as the hydroxy group of **19** and the amino group of Gly331 (1.84 Å). In addition, the carbonyl group of **19** can form another hydrogen bond with the –NH belonging to the imidazole moiety of His198

Table 2 In silico histone deacetylase inhibitory activity of the selected compounds

Compounds	Class I HDACs				Class II HDACs			
	HDAC2		HDAC8		HDAC4		HDAC7	
	Δ*G* (kcal/mol)	K_i (μM)	Δ*G* (kcal/mol)	K_i	Δ*G* (kcal/mol)	K_i (μM)	Δ*G* (kcal/mol)	K_i (μM)
SAHA	−9.38	0.13	−0.74	1.78	−0.51	3.14	−0.70	12.36
TSA	−0.75	0.39	−0.85	0.326	−0.39	0.702	−0.97	1.44
6	−0.85	9.54	−0.46	18.38	−0.80	1.91	−0.79	10.63
10	−0.19	0.98	−0.95	8.01	−0.62	13.99	−7.61	2.64
19	−0.4	20.23	−0.37	3.97	−0.74	2.11	−0.93	8.26

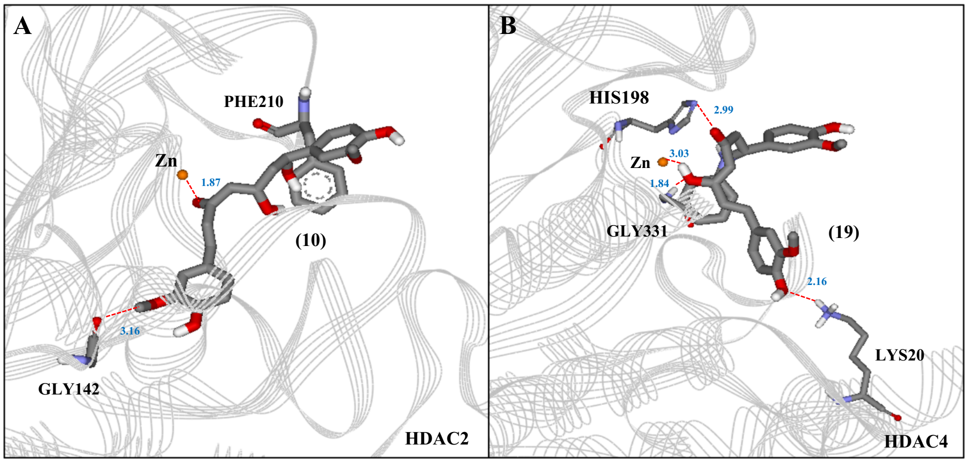

Fig. 3 The interaction modes of **a** **10** in the active site cavity of HDAC2 and **b** **19** in the active site cavity of HDAC4

Table 3 In vitro antioxidant activities of the compounds

Compounds	DPPH[a]	RP[b]	TA[b]	Compounds	DPPH[a]	RP[b]	TA[b]
6	6	11	43	**13**	5	10	28
7	11	16	45	**14**	8	30	28
8	7	12	46	**15**	7	22	35
9	11	25	60	**16**	14	15	54
10	24	12	52	**17**	6	15	38
11	7	22	51	**18**	6	10	39
12	5	17	30	**19**	7	14	42

[a]IC_{50} (μM) [b]EC_{50} (μM)

(2.99 Å). The π–π interaction can also be observed between the imidazole of His198 and the newly inserted aminophenyl group of **19**. The histidine residues are important in the mechanism of histone deacetylation as the zinc-ion chelator. They also catalyze deprotonation of water molecules to generate nucleophiles which can attack the acetylated lysine residues of histones as proposed (Bertrand 2010; Manal et al. 2016). Therefore, the HDAC inhibitors which can form strong interactions with the histone residues will definitely reduce the binding affinity between co-factor, natural substrate and enzymes. The class IIa HDAC inhibitors are considered as a potential therapy for Huntington's disease (Bürli et al. 2013), so the HDAC4 selective inhibitor, compound **19**, should be further investigated. The progression of multiple neurodegenerative diseases such as Alzheimer's and Huntington's diseases relates to oxidative stress which causes by the increased production of reactive oxygen species (Tönnies and Trushina 2017). To explore the antioxidative potency of the obtained HDAC inhibitors, the antioxidant activities were tested and compound **19** appeared to be a good antioxidant as displayed in Table 3.

Finally, the MTT assay was carried out to gain more details regarding the anticancer activities of the potent HDAC inhibitors. The results in Tables 4 and 5 indicate that the amino derivatives of curcumin **16**–**19** were less toxic to non-cancer cells than the lead compound, even though curcumin (**6**) was the most active against all cancer cells. Compound **17**, the least toxic compound, showed the best activity against HeLa cells among the synthesized derivatives. Moreover, compound **17** appeared to be about 16-fold more selective towards the cancer cells than the non-cancer cells, whereas curcumin (**6**) exhibited only three-fold selectivity. Compounds **18** and **19** were the most potent derivatives against MCF-7 and HCT116 cells, respectively. Additionally, compound **18** displayed the strongest antiproliferative activity against the cholangiocarcinoma cells as shown in Table 5. The least toxic compound against non-cancer human bile-duct epithelial cells, compound **19**, exhibited antiproliferative activity against cholangiocarcinoma cells without selectivity.

Table 4 Antiproliferative activities of the potent HDAC inhibitors against cancer cell lines

Cpd	IC_{50} values (mean ± SD; $n = 3$ (μg/mL)											
	Vero cells			Hela cells			HCT116 cells			MCF-7 cells		
	24 h	48 h	72 h	24 h	48 h	72 h	24 h	48 h	72 h	24 h	48 h	72 h
6	25.00 ± 1.11	17.87 ± 2.65	10.97 ± 0.80	5.39 ± 0.20	3.57 ± 0.50	3.56 ± 0.47	3.83 ± 0.07	2.67 ± 0.20	2.40 ± 0.15	2.94 ± 0.46	2.08 ± 0.12	2.03 ± 0.16
16	74.31 ± 4.21	26.09 ± 1.28	15.97 ± 1.47	19.12 ± 0.17	9.96 ± 0.57	9.15 ± 0.62	21.09 ± 2.40	11.98 ± 0.77	8.36 ± 0.83	15.37 ± 0.67	11.66 ± 0.80	10.32 ± 0.14
17	>100	>100	80.64 ± 4.88	9.06 ± 0.76	6.55 ± 0.13	4.69 ± 0.14	9.06 ± 0.76	6.55 ± 0.13	4.69 ± 0.14	6.72 ± 0.25	6.15 ± 0.26	5.23 ± 0.21
18	>100	43.58 ± 6.93	11.62 ± 1.26	10.37 ± 0.79	6.63 ± 0.81	5.50 ± 0.12	7.95 ± 1.04	4.54 ± 0.13	3.80 ± 0.39	5.92 ± 0.28	5.30 ± 0.02	4.58 ± 0.26
19	>100	23.16 ± 0.92	16.29 ± 0.42	29.13 ± 0.86	14.99 ± 0.48	12.81 ± 0.31	9.04 ± 0.54	8.30 ± 0.78	2.97 ± 0.06	18.06 ± 1.27	15.32 ± 0.39	13.27 ± 1.49

Table 5 Antiproliferative activities of the potent HDAC inhibitors against cholangiocarcinoma cell lines

Cpd	IC_{50} values (mean ± SD; $n = 3$ (μg/mL)								
	H-69 cells			KKU-100 cells			KKU-M214 cells		
	24 h	48 h	72 h	24 h	48 h	72 h	24 h	48 h	72 h
6	4.59 ± 0.29	2.54 ± 0.09	2.37 ± 0.14	27.79 ± 0.93	3.28 ± 0.37	2.88 ± 0.14	6.95 ± 1.61	3.80 ± 0.06	3.64 ± 0.20
16	22.98 ± 5.31	12.96 ± 2.02	9.94 ± 0.44	43.17 ± 6.56	14.29 ± 0.70	10.53 ± 1.02	28.04 ± 2.96	21.72 ± 1.82	14.55 ± 0.55
17	12.54 ± 3.21	8.92 ± 0.81	6.39 ± 1.13	> 100	17.15 ± 1.19	10.55 ± 0.27	33.96 ± 2.26	8.63 ± 0.35	7.00 ± 0.47
18	15.43 ± 1.30	8.13 ± 0.06	6.62 ± 0.29	80.33 ± 9.66	6.63 ± 0.81	5.50 ± 0.12	26.94 ± 0.70	6.84 ± 1.08	5.50 ± 0.37
19	23.58 ± 0.56	19.49 ± 0.61	17.37 ± 0.25	42.15 ± 0.59	19.93 ± 0.29	17.96 ± 0.42	37.71 ± 1.00	19.55 ± 1.76	17.39 ± 0.33

Numerous analogs of curcumin have been developed for therapeutic purposes especially modification around β-diketo scaffold. The replacement of β-diketo unit in curcumin by isoxazole and pyrazole moieties can enhance some biological activities and maintain their low toxicity. However, there was unprecedented modification at the α, β-unsaturated carbonyl group. Our newly synthesized Michael-adduct derivatives of curcumin (**16**–**19**) performed stronger HDAC inhibitory activity than curcumin (**6**), the isoxazole derivative (**11**) and the pyrazole derivatives (**12**–**15**). Variety of nucleophiles could be introduced into the Micael-acceptor curcumin in order to improve the inhibitor-enzyme binding. This finding suggests another simple approach to enhance biological activity for chemotherapeutic application of a golden spice from mother nature.

Conclusion

C. longa could serve as a great source of HDAC inhibitors with partial isoform-selectivity. The core-structure modification of the natural compound, curcumin (**6**) provided the series of derivatives with improved activities. The cytotoxic activity of the active HDAC inhibitors might not increase dramatically compared to the lead compound; however, the non-toxicity of those compounds was promising. Therefore, the in vivo experiments of the potent HDAC inhibitors will be further investigated.

Experimental

Reagents were purchased from commercial sources (Sigma-Aldrich, Merck, and Carlo Erba). Reactions were monitored using analytical TLC plates (Merck, silica gel 60 F_{254}) and compounds were visualized under ultraviolet light. Silica gel grade 60 (230–400 mesh; Merck) was used for column chromatography. The NMR spectra were recorded in the individually indicated solvents on a Varian Mercury Plus spectrometer operated at 400 MHz (^{1}H) or 100 MHz (^{13}C). The IR spectra were obtained on Perkin Elmer Spectrum One FT-IR spectrophotometer. Mass spectra were determined using a Micromass Q-TOF 2 hybrid quadrupole time-of-flight (Q-TOF) mass spectrometer with a Z-spray ES source.

Plant material

The dried rhizome powder of turmeric was obtained from the herbal drugstore at local market in Khon Kaen province, Thailand. The powder was confirmed by a pharmacist as *C. longa*.

Extraction and isolation

Six hundred grams of plant material were extracted three times (3 × 1000 mL) with dichloromethane (CH_2Cl_2). The combinded extracts were evaporated to dryness under vacuum to give the dichloromethane extract (90 g). The dichloromethane extract was further isolated with normal phase silica gel column chromatography and subsequently eluted with three solvents (hexane, ethyl acetate (EtOAc), and methanol (MeOH)) by gradually increasing polarity of elution solvent system. The eluents were collected and monitored by TLC to afford four fractions (DT_1–DT_4). The fraction DT_1 was an oil. The fraction DT_2 was resolved by flash silica gel column chromatography, using a gradient of hexane-EtOAc (10:0 to 5:5) to provide three subfractions (DT_{2-1} to DT_{2-3}). The subfraction DT_{2-1} and DT_{2-2} were purified by preparative thin layer chromatography (hexane-EtOAC, 9:1) to obtain demethoxycurcumin (**7**, 0.05 g, 0.0083%) and dihydrocurcumin (**8**, 0.04 g, 0.00067%) as a yellow solid. The fraction DT_{2-3} was subjected to normal phase silica gel column chromatography, eluting with an isocratic of CH_2Cl_2-MeOH (9:1) to afford curcumin (**6**, 20 g, 3.33%) as an orange solid. The fraction DT_3 was further subjected to a normal phase silica gel column, eluting with a step gradient of CH_2Cl_2-MeOH (10:0 to 7:3) to yield two subfractions (DT_{3-1} and DT_{3-2}). The subfraction DT_{3-2} was subjected to a normal phase column chromatography, eluting with an isocratic of CH_2Cl_2-MeOH (9:1) to produce bisdemethoxycurcumin (**9**, 1.0 g, 0.167%).

The fraction DT$_4$ was isolated with a normal phase silica gel column, eluting with a step gradient of CH$_2$Cl$_2$-MeOH (10:0 to 7:3) to yield two subfractions (DT$_{4–1}$ and DT$_{4–2}$). The subfraction DT$_{4–1}$ and DT$_{4–2}$ were further purified by preparative thin layer chromatography (CH$_2$Cl$_2$-MeOH, 9:1) to gain hydroxycurcumin (**10**, 0.012 g, 0.002%). The NMR data of all compounds were consistent with the previous report (Venkateswarlu et al. 2005).

Structural modifications

To a solution of curcumin (**6**) (105 mg, 0.29 mmol) in ethanol (5 mL) was added NH$_2$OH·HCl (40 mg, 0.57 mmol) at room temperature. The mixture was refluxed for 6 h. After completion based on TLC, the mixture was filtered and the residue was washed with ethanol (10 mL) and dried with anhydrous sodium sulfate. Evaporation of the combined solvents gave a crude product. Purification of the crude product by column chromatography (5% MeOH in CH$_2$Cl$_2$) gave a yellow solid of compound **11**. The same procedure was applied with the corresponding reagents to convert curcumin (**6**) into **12**–**15**. The NMR of all synthesized compounds were in consistency with the earlier reports (Mishra et al. 2008; Sahu et al. 2012; Jha et al. 2015; Jordan et al. 2018).

To a solution of curcumin (**6**) (100 mg, 0.27 mmol) in ethanol (5 mL) was added NH$_2$OCH$_3$·HCl (34 mg, 0.41 mmol) at room temperature. The mixture was refluxed for 6 h. After completion based on TLC, the mixture was filtered and the residue was washed with ethanol (10 mL) and dried with anhydrous sodium sulfate. Evaporation of the combined solvents gave a crude product. Purification of the crude product by column chromatography (5% MeOH in CH$_2$Cl$_2$) gave a yellow solid of compound **16**. The same procedure was conducted with 2-aminothiophenol, *o*-phenylenediamine, and aniline to convert curcumin (**6**) into **17**–**19**.

(4*Z*,6*E*)-5-Hydroxy-1,7-bis(4-hydroxy-3-methoxyphenyl)-1-(methoxyamino)hepta-4,6-dien-3-one (**16**): 80%. R_f = 0.70 (10% MeOH in CH$_2$Cl$_2$). IR (neat) υ_{max} 3272 (OH), 1734 (C = O), 1583 (Ar), 1511 (Ar), 1273 (C–O) cm^{-1}.^{1}H NMR (CDCl$_3$, 400 MHz) δ 7.16 (d, J = 16.0 Hz, 1H$_7$), 7.05 (dd, J = 2.0, 8.0 Hz, 1H$_{2''}$), 6.93 (m, 5H, aromatic), 6.74 (d, J = 16.0 Hz, 1H$_6$), 5.58 (s, 1H$_4$), 4.68 (dd, J = 4.0, 8.0 Hz, 1H$_1$), 3.91 (s, OCH$_3$), 3.90 (s, OCH$_3$), 3.40 (s, 3H$_{1'''}$), 2.90 (dd, J = 16.0, 16.0 Hz, 1H$_2$), 2.73 (dd, J = 4.0, 16.0 Hz, 1H$_2$). ^{13}C NMR (CDCl$_3$, 100 MHz) δ 192.02 (C-3), 164.70 (C-5), 147.34 (C-3″), 146.83 (C-4″), 146.47 (C-3′), 145.84 (C-4′), 137.52 (C-7), 129.52 (C-1″), 128.23 (C-1′), 121.68 (C-6″), 121.27 (C-6′), 117.35 (C-5″), 114.89 (C-5′), 114.38 (C-2″), 110.68 (C-2′), 109.56 (C-6), 100.47 (C-4), 67.33 (C-1), 63.30 (C-1‴), 56.00 (OCH$_3$), 44.95 (C-2). HRMS-ESI (*m/z*) [M –H$_2$O + H]$^+$ calcd for C$_{22}$H$_{24}$NO$_6$ 398.1603, found 398.1617.

(4*Z*,6*E*)-5-Hydroxy-1,7-bis(4-hydroxy-3-methoxyphenyl)-1-((2-mercaptophenyl)amino)hepta-4,6-dien-3-one (**17**): 82%. R_f = 0.50 (5% MeOH in CH$_2$Cl$_2$). IR (neat) υ_{max} 3288 (OH), 1738 (C = O), 1560 (Ar), 1508 (Ar), 1265 (C–O) cm^{-1}.^{1}H NMR (CDCl$_3$, 400 MHz) δ 7.54 (dd, J = 2.0, 8.0 Hz, 1H, aromatic), 7.39 (m, 2H, aromatic), 7.14 (m, 3H, aromatic), 7.01 (dd, J = 2.0, 8.0 Hz, 1H, aromatic), 6.90 (s, 1H, aromatic), 6.76 (d, J = 8.0 Hz, 1H, aromatic), 6.69 (s, 2H, aromatic), 6.63 (d, J = 12.0 Hz, 1H$_6$), 5.48 (s, 1H$_4$), 4.71 (dd, J = 4.0, 8.0 Hz, 1H$_1$), 3.83 (s, OCH$_3$), 3.72 (s, OCH$_3$), 2.75 (dd, J = 4.0, 12.0 Hz, 1H$_2$), 2.61 (dd, J = 8.0, 12.0 Hz, 1H$_2$). ^{13}C NMR (CDCl$_3$, 100 MHz) δ 188.55 (C-3), 161.57 (C-5), 149.78 (C-3″), 148.22 (C-4″), 147.47 (C-3′), 145.96 (C-4′), 141.75 (C-1‴), 139.95 (C-7), 135.02 (C-1″), 134.98 (C-1′), 129.94 (C-3‴), 126.77 (C-6‴), 126.74 (C-5‴), 125.93 (C-6″), 124.43 (C-6′), 123.17 (C-4‴), 122.53 (C-5″), 119.03 (C-5′), 115.42 (C-2‴), 114.66 (C-2″), 110.26 (C-2′), 110.12 (C-6), 98.00 (C-4), 55.01 (C-1), 54.92 (OCH$_3$), 40.15 (C-2). HRMS-ESI (*m/z*) [M –H$_2$O + H]$^+$ calcd for C$_{27}$H$_{26}$NO$_5$S 476.1531, found 476.1574.

(4*Z*,6*E*)-1-((2-Aminophenyl)amino)-5-hydroxy-1,7-bis(4-hydroxy-3-methoxyphenyl)hepta-4,6-dien-3-one (**18**): 85%. R_f = 0.55 (5% MeOH in CH$_2$Cl$_2$). IR (neat) υ_{max} 3296 (OH), 1738 (C = O), 1571 (Ar), 1508 (Ar), 1270 (C–O) cm^{-1}.^{1}H NMR (CDCl$_3$, 400 MHz) δ 7.36 (d, J = 16.0 Hz, 1H$_7$), 7.15 (d, J = 2.0 Hz, 1H, aromatic), 7.02 (m, 4H, aromatic), 6.95 (d, J = 8.0 Hz, 1H, aromatic), 6.89 (m, 1H, aromatic), 6.76 (m, 4H, aromatic), 6.61 (d, J = 16.0 Hz, 1H$_6$), 3.88 (s, OCH$_3$), 3.79 (s, OCH$_3$), 2.78 (dd, J = 4.0, 8.0 Hz, 1H$_2$), 2.67 (dd, J = 4.0, 16.0 Hz, 1H$_2$). ^{13}C NMR (CDCl$_3$, 100 MHz) δ 187.15 (C-3), 162.36 (C-5), 149.22 (C-3″), 148.12 (C-4″), 147.53 (C-3′), 145.75 (C-4′), 139.83 (C-7), 138.85 (C-1′), 136.19 (C-1″& C-2‴), 127.94 (C-1‴), 127.12 (C-6″), 125.74 (C-6′), 124.65 (C-5‴), 122.34 (C-4‴), 122.27 (C-6‴), 120.45 (C-5″), 120.33 (C-5′), 118.56 (C-2′), 115.25 (C-2″), 114.63 (C-3‴), 110.08 (C-6), 109.73 (C-4), 64.97 (C-1), 54.98 (OCH$_3$), 40.44 (C-2). HRMS-ESI (*m/z*) [M –H$_2$O + H]$^+$ calcd for C$_{27}$H$_{27}$N$_2$O$_5$ 459.1920, found 459.1970.

(4*Z*,6*E*)-5-Hydroxy-1,7-bis(4-hydroxy-3-methoxyphenyl)-1-(phenylamino)hepta-4,6-dien-3-one (**19**): 80%. R_f = 0.40 (5% MeOH in CH$_2$Cl$_2$). IR (neat) υ_{max} 3355 (OH), 1736 (C = O), 1509 (Ar), 1457 (Ar), 1271 (C–O) cm^{-1}.^{1}H NMR (CDCl$_3$, 400 MHz) δ 7.27 (m, 5H, aromatic), 7.10 (d, J = 8.0 Hz, 2H, aromatic), 6.79 (m, 3H, aromatic), 6.74 (m, 2H, aromatic), 6.21 (d, J = 16.0 Hz, 1H$_6$), 5.63 (s, 1H$_4$), 5.09 (dd, J = 4.0, 8.0 Hz, 1H$_1$), 3.77 (s, OCH$_3$), 3.25 (dd, J = 8.0, 16.0 Hz, 1H$_2$), 2.74 (dd, J = 4.0, 16.0 Hz, 1H$_2$). ^{13}C NMR (CDCl$_3$, 100 MHz) δ 191.55 (C-3), 161.32 (C-5), 148.39 (C-1‴), 147.79 (C-3″), 147.72 (C-4″), 145.87 (C-3′), 143.63 (C-4′), 138.59 (C-7), 130.16 (C-1″), 129.08 (C-1′), 127.33 (C-6″), 126.82 (C-6′), 125.98 (C-3‴), 121.56 (C-4‴), 119.58 (C-5″), 119.40 (C-5′), 115.33 (C-2‴), 115.06 (C-2″), 110.26 (C-2′), 110.09 (C-6), 97.71 (C-4), 65.03 (C-1), 55.41 (OCH_3), 42.45 (C-2). HRMS-ESI (*m/z*) $[M - H_2O + H]^+$ calcd for $C_{27}H_{26}NO_5$ 444.1811, found 444.1870.

HDAC activity assay

Natural compounds and the semi-synthetic derivatives were evaluated for their ability to inhibit HDAC enzymes. Inhibition of HDAC activity in vitro was assessed using the Fluor-de-Lys HDAC activity assay kit (Biomol, Enzo Life Sciences International, Inc., USA). The HeLa nuclear extract provided with the kit was used as a source of HDAC enzymes for in vitro study. TSA was used as the positive control. The HeLa nuclear extract, substrate, buffer, and inhibitors were incubated. Deacetylation of the substrate followed with adding the developer generated a fluorophore. The spectra Max Gemini XPS microplate spectrofluorometer (Molecular Devices, USA) was used to measure fluorescence signal with excitation at 360 nm and emission at 460 nm. A decrease in fluorescence signal indicated an inhibition of HDAC activity. All experiments were carried out in triplicate.

MTT assay

The MTT reduction assay was performed with non-cancer (Vero), human cervical cancer (HeLa), human colon cancer (HCT116), human breast adenocarcinoma cancer (MCF-7), non-cancer human bile-duct epithelial (H-69), and cholangiocarcinoma (KKU-100 and KKU-M214) cell lines according to the method previously described (Senawong et al. 2015; Asgar et al. 2016; Kumnerdkhonkaen et al. 2018). Briefly, cells were seeded into 96-well plates. The next day, cells were exposed to the selected compounds at various concentrations and incubated for 24, 48, and 72 h. After incubation, the culture medium was exchanged with 110 µL of MTT (0.5 mg/mL in PBS medium) and further incubated for 2 h. The amount of MTT formazan product was determined after dissolved in DMSO by measuring its absorbance with a microplate reader (Bio-Rad Laboratories, USA) at a test wavelength of 550 nm and a reference wavelength of 655 nm. The cell viability was expressed as a percentage to the viable cells of control culture condition and IC_{50} values of each group were calculated.

Molecular docking studies

The crystal structures of HDAC2, HDAC4, HDAC7, and HDAC8 [PDB entry code: 3MAX, 2VQW, 3C0Z, and 1T64, respectively] were obtained from the Protein Data Bank (available from http://www.rcsb.org, last accessed 30 October 2015). All water and non-interacting ions as well as ligands were removed. Then, all missing hydrogen and side-chain atoms were added using the ADT program. Gasteiger charges were calculated for the system. For ligand setup, the molecular modeling program Hyperchem 8.0 was used to build the ligands. These ligands were optimized with the AM1 level. Molecular docking studies were performed for 50 runs using AutoDockTools 1.5.4 (ADT) and AutoDock 4.2 programs and Lamarckian genetic algorithm search (Sanner 1999). A grid box size of 60 ×60 × 60 points with a spacing of 0.375 Å between the grid points was implemented and covered almost the entire HDAC protein surface. For TSA and other inhibitors, the single bonds were treated as active torsional bonds.

DPPH radical scavenging

The antioxidant activity of the obtained compounds were measured in terms of hydrogen-donating or radical scavenging ability, using the DPPH method (Kumboonma et al. 2017). Gallic acid was used as a positive control. Different concentrations (1 mL) of the above compounds were mixed with 3 mL DPPH radical solution in methanol (1.0×10^{-4} M). The final concentration of DPPH reached 0.6×10^{-4} M with methanol. The reaction mixtures were shaken and incubated at room temperature for 30 min. At the same time, the control was prepared as mentioned above without any compounds. The absorbance of the solution was measured at 517 nm. Radical scavenging activity was expressed as the inhibition percentage and was calculated via the following formula:

$$\begin{aligned}&\%\ \text{Radical scavenging activity}\\&= \left[\left(\text{Abs}_{\text{control}} - \text{Abs}_{\text{sample}}\right)/\text{Abs}_{\text{control}}\right] \times 100.\end{aligned}$$

The decoloration was plotted against the samples, and a logarithmic regression curve was established in order to calculate the IC_{50} which is the amount of sample necessary to decrease by 50% the absorbance of DPPH. All experiments were carried out in triplicate. The IC_{50} value of gallic acid was obtained as 21 µM which related to the previous report (Assaashari et al. 2014).

Reducing power

The reducing power of the obtained compounds was determined by the Fe(III)-reduction (Oktay et al. 2003). Different concentrations of the sample in DMSO 1 mL were mixed with 0.2 M phosphate buffer (pH 6.6, 2.5 mL) and 1% (v/v) potassium ferricyanide (2.5 mL). The mixture was incubated at 50 °C for 20 min. A portion (2.5 mL) of 10% trichloroacetic acid was added to the mixture which was then centrifuged at 3000 r.p.m. for 10 min. The upper layer of solution 2.5 mL was mixed with DI water 2.5 mL and 0.5 mL of 0.1% $FeCl_3$. The absorbance was measured at

700 nm using a spectrophotometer. Ascorbic acid was used as a positive control. The reducing power was displayed by effective concentration of 0.5 absorbance. All experiments were carried out in triplicate. Ascorbic acid showed the EC_{50} value of 9 μM. The earlier study indicated the value to be about 13 μM (Berber et al. 2014).

Total antioxidant capacity

The total antioxidant capacity of the obtained compounds was determined by the phosphomolybdenum method (Oktay et al. 2003). Different concentrations of the samples in DMSO (1 mL) were mixed with 1 mL of reagent solution (0.6 M H_2SO_4, 28 mM sodium phosphate, and 4 mM ammonium molybdate). Next, the tubes were covered and incubated in a water bath at 95 °C for 90 min. After that, the tubes were cooled to room temperature and the absorbance was measured at 695 nm using a spectrophotometer. Ascorbic acid was used as a positive control. The total antioxidant capacity was expressed by effective concentration of 0.5 absorbance. All experiments were carried out in triplicate. The standard ascorbic acid displayed the EC_{50} value of 66 μM.

Acknowledgements Khon Kaen University is gratefully acknowledged for the financial support of this work (Grant Number 6200014002). We also would like to thank Mr. Kittisak Poopasith for the excellent NMR data. We are thankful to the Postdoctoral Training Program, Graduate School, Khon Kaen University for providing a fellowship to Dr. Somprasong Saenglee. A graduate fellowship given to Pakit Kumboonma and La-or Somsakeesit is supported by Rajamangala University of Technology Isan (RMUTI).

Compliance with ethical standards

Conflict of interest The authors declare that they have no conflict of interest.

References

Ahsan MJ, Choudhary K, Jadav SS, Yasmin S, Ansari MY, Sreenivasulu R (2015) Synthesis, antiproliferative activity, and molecular docking studies of curcumin analogues bearing pyrozole ring. Med Chem Res 24:4166–4180

Anand P, Thomas SG, Kunnumakkara AB, Sundaram C, Harikumar KB, Sung B et al. (2008) Biological activities of curcumin and its analogues (congeners) made by man and mother nature. Biochem Pharm 76:1590–1611

Asgar MA, Senawong G, Sripa B, Senawong T (2016) Synergistic anticancer effects of cisplatin and histone deacetylase inhibitors (SAHA and TSA) on cholangiocarcinoma cell lines. Int J Oncol 48:409–420

Assaashari M, Farhoosh R, Sharif A (2014) Antioxidnt activity of gallic acid and methyl gallate in triacylglycerols of kika fish oil and its oil-in-water emulsion. Food Chem 159:439–444

Banerjee S, Adhikari N, Amin SA, Jha T (2019) Histone deacetylase 8 (HDAC8) and its inhibitors with selectivity to other isoforms: an overview. Eur J Med Chem 164:214–240

Berber A, Zengin G, Aktumsek A, Sanda MA, Uysal T (2014) Antioxidant capacity and fatty acid composition of different parts of Adenocarpus complicates (Fabaceae) from Turkey. Rev Biol Trop 62:337–346

Bertrand P (2010) Inside HDAC with HDAC inhibitors. Eur J Med Chem 45:2095–2116

Bürli RW, Luckhurst CA, Aziz O, Matthews KL, Yates D, Lyons KA et al. (2013) Design, synthesis, and biological evaluation of potent and selective class Iia histone deacetylase (HDAC) inhibitors as a potential therapy for Huntington's disease. J Med Chem 56:9934–9954

Chan MMY, Ho CT, Huang HI (1995) Effects of three dietary phytochemicals from tea, rosemary and turmeric on inflammation-induced nitrite production. Cancer Lett 96:23–29

Changtam C, Hongmanee P, Suksamrarn A (2010) Isoxazole analogs of curcuminoids with highly potent multidrug-resistant antimycobacterial. Eur J Med Chem 45:4446–4457

Gopalan B, Ponpandian T, Kachhadia V, Bharathimohan K, Vignesh R, Sivasudar V, Narayanan S, Mandar B, Praveen R, Saranya N, Rajagopal S, Rajagopal S (2013) Discovery of adamantane based highly potent HDAC inhibitors. Bioorg Med Chem Lett 23:2532–2537

Hahnen E, Hauke J, Trankle C, Eyupoglu IY, Wirth B, Blumcke I (2008) Histone deacetylase inhibitors: possible implications for neurodegenerative disorders. Expert Opin Invest Drugs 17:169–184

Hu J, An B, Pan T, Li Z, Huang L, Li X (2018) Design, synthesis, and biological evaluation of histone deacetylase inhibitors possessing glutathione peroxidase-like and antioxidant activities against Alzheimer's disease. Bioorg Med Chem 26:5718–5729

Inano H, Onoda M, Inafugu N, Kubota M, Kamada Y, Osawa T, Kobayashi H, Wakabayashi K (2000) Potent preventive action of curcumin on radiation-induced initiation of mammary tumorigenesis in rats. Carcinogenesis 21:1835–1841

Jha NS, Mishra S, Jha SK, Surolia A (2015) Antioxidant activity and electrochemical elucidation of the enigmatic redox behavior of curcumin and its structurally modified analogues. Electro Acta 151:574–583

Jordan BC, Kumar B, Thilagavathi R, Yadhav A, Kumar P, Selvam C (2018) Synthesis, evaluation of cytotoxic properties of promising curcumin analogues and investigation of possible molecular mechanisms. Chem Biol Drug Des 91:332–337

Khalil MI, AL-Zahem AM, Qunaibit MM (2014) Synthesis, characterization, and antitumor activity of binuclear curcumin-metal (II) hydroxo complexes. Med Chem Res 23:1683–1689

Konstantinopoulos PA, Karamouzis MV, Papavassiliou AG (2007) Focus on acetylation: the role of histone deacetylase inhibitors in cancer therapy and beyond. Expert Opin Invest Drugs 16:569–571

Kumboonma P, Senawong T, Saenglee S, Yenjai C, Phaosiri C (2017) Identificaton of phenolic compounds from *Zingiber offinale* and their derivatives as histone deacetylase inhibitors and antioxidants. Med Chem Res 26:650–661

Kumnerdkhonkaen P, Saenglee S, Asgar MA, Senawong G, Khongsukwiwat K, Senawong T (2018) Antiproliferative activities and phenolic acid content of water and ethanolic extracts of the powdered formula of *Houttuynia cordata* Thunb. fermented broth and *Phyllanthus emblica* Linn. fruit. BMC Complement Altern Med 18:130–132

Manal M, Chandrasekar MJN, Priya JG, Nanjan MJ (2016) Inhibitors of histone deacetylase as antitumor agents: a critical review. Bioorg Chem 67:18–42

Mann BS, Johnson JR, Cohen MH, Justice R, Pazdur R (2007) FDA approval summary: vorinostat for treatment of advanced primary cutaneous T-cell lymphoma. Oncologist 12:1247–1252

Mazumder A, Raghavan K, Weinstein L, Kohn KW, Pommier Y (1995) Inhibition of human immunodeficiency virus type-1 integrase by curcumin. Biochem Pharm 49:1165–1170

Micelli C, Rastelli G (2015) Histone deacetylases: structural determinants of inhibitor selectivity. Drug Discov Today 20:718–735

Miller TA, Witter DJ, Belvedere S (2003) Histone deacetylase inhibitors. J Med Chem 46:5097–5116

Mishra S, Karmodiya K, Surolia N, Surolia A (2008) Synthesis and exploration of novel curcumin analogues as anti-malarial agents. Bioorg Med Chem 16:2894–2902

Noh H, Oh EY, Seo JY, Yu MR, Kim YO, Ha H (2009) Histone deacetylase-2 is a key regulator of diabetes and transforming growth factor-β1-induced renal injury. Am J Physiol Ren Physiol 207:729–739

Oktay M, Gulcin I, Kufrevioglu OI (2003) Determination of in vitro antioxidant activity of fennel (*Foeniculum vulgare*) seed extracts. Leb Wiss Technol 36:263–271

Ontoria JM, Altamura S, Marco AD, Ferrigno F, Laufer R, Muraglia E, Palumbi MC, Rowley M, Scarpelli R, Fademrecht CS, Serafini S, Steinkühler C, Jones P (2009) Identification of novel, selective, and stable inhibitors of class II histone deacetylases. Validation studies of the inhibition of the enzymatic activity of HDAC4 by small molecules as a novel approach of cancer therapy. J Med Chem 52:6782–6789

Paris M, Porcelloni M, Binaschi M, Fattori D (2008) Histone deacetylase inhibitors: from bench to clinic. J Med Chem 51:1505–1529

Premanand C, Rema M, Sameer MZ, Sujatha M, Balasubramanvam M (2009) Inhibitory effect of curcuminoids on acetylcholinesterase activity and attenuation of scopolamine-induced amnesia may explain medicinal use of turmeric in Alzheimer's disease. Pharm Biochem Behav 91:554–559

Puneeth HR, Ananda H, Kumar KSS, Rangappa KS, Sharada AC (2016) Synthesis and antiproliferative studies of curcumin pyrazole derivatives. Med Chem Res 25:1842–1851

Ravichandiran P, Jegan A, Premnath D, Periasamy VS, Vasanthkumar S (2015) Design, synthesis, molecular docking as histone deacetylase (HDAC8) inhibitors, cytotoxicity and antibacterial evaluation of novel 6-(4-(4-aminophenylsulfonyl)phenylamino)-5*H*-benzo[*a*] phenoxazin-5-one derivatives. Med Chem Res 24:197–208

Ruby AJ, Kuttan G, Babu KD, Rajasekharan KN, Kuttan R (1995) Anti-tumour and antioxidant activity of natural curcuminoids. Cancer Lett 94:79–83

Sahu PK, Sahu PK, Gupta SK, Thavaselvam D, Agarwal DD (2012) Synthesis and evaluation of antimicrobial activity of 4*H*-pyrimido [2,1-*b*] benzothiazole, pyrazole and benzylidene derivatives of curcumin. Eur J Med Chem 54:366–378

Sanner MF (1999) Python: a programming language for software integration and development. J Mol Graph Model 17:57–61

Selvam C, Jachak SM, Thilagavathi R, Chakraborti AK (2005) Design, synthesis, biological evaluation and molecular docking of curcumin analogues as antioxidant, cyclooxygenase inhibitory and anti-inflammatory agents. Bioorg Med Chem Lett 15:1793–1797

Senawong T, Wongphakham P, Saiwichai T, Phaosiri C, Kumboonma P (2015) Histone deacetylase inhibitory activity of hydroxycapsaicin, a synthetic derivative of capsaicin, and its cytotoxic effects against human colon cancer cell lines. Turk J Biol 39:1–10

Sharma R, Jadav SS, Yasmin S, Bhatia S, Khalilullah H, Ahsan MJ (2015) Simple, efficient, and improve synthesis of Biginelli-type compounds of curcumin as anticancer agents. Med Chem Res 24:636–644

Suzuki T, Miyata N (2005) Non-hydroxamate histone deacetylase inhibitors. Curr Med Chem 12:2867–2880

Tatar GB, Erden DD, Demir AS, Dalkara S, Yelekci K, Yurter HE (2009) Molecular modifications on carboxylic acid derivatives as potent histone deacetylase inhibitors: activity and docking studies. Bioorg Med Chem 17:5219–5228

Thapliyal R, Maru GB (2001) Inhibition of Cytochrome P450 isozymes by curcumins in vitro and in vivo. Food Chem Toxicol 39:541–547

Tönnies E Trushina E (2017) Oxidative stress,synaptic dysfunction, and Alzheimer’s disease. J Alzheimer Dis 57:1105–1121

Venkateswarlu S, Ramachandra MS, Subbaraju GV (2005) Synthesis and biological evaluation of polyhydroxycurcuminoids. Bioorg Med Chem 13:6374–6380

Weichert W (2009) HDAC expression and clinical prognosis inhuman malignancies. Cancer Lett 280:168–176

Zhang L, Minyong L, Jinhong F, Hao F, Wenfang X (2012) Discovery of a novel histone deacetylase 8 inhibitor. Med Chem Res 21:152–156